Experimental Mechanics (2010) 50:1275–1281
DOI 10.1007/s11340-009-9267-0

The Dilute Rheology of Swimming Suspensions: A Simple Kinetic Model

D. Saintillan

Received: 30 March 2009 / Accepted: 11 June 2009 / Published online: 30 June 2009

Abstract A simple kinetic model is presented for the shear rheology of a dilute suspension of particles swimming at low Reynolds number. If interparticle hydrodynamic interactions are neglected, the configuration of the suspension is characterized by the particle orientation distribution, which satisfies a Fokker-Planck equation including the effects of the external shear flow, rotary diffusion, and particle tumbling. The orientation distribution then determines the leading-order term in the particle extra stress in the suspension, which can be evaluated based on the classic theory of Hinch and Leal (J Fluid Mech 52(4):683–712, 1972), and involves an additional contribution arising from the permanent force dipole exerted by the particles as they propel themselves through the fluid. Numerical solutions of the steady-state Fokker-Planck equation were obtained using a spectral method, and results are reported for the shear viscosity and normal stress difference coefficients in terms of flow strength, rotary diffusivity, and correlation time for tumbling. It is found that the rheology is characterized by much stronger normal stress differences than for passive suspensions, and that tail-actuated swimmers result in a strong decrease in the effective shear viscosity of the fluid.

Keywords Microorganisms · Suspensions · Swimming · Rheology

D. Saintillan (✉)
Department of Mechanical Science and Engineering,
University of Illinois at Urbana-Champaign,
Urbana, IL 61801, USA
e-mail: dstn@illinois.edu

Introduction

Suspensions of self-propelled particles, of which swimming microorganisms are a paradigmatic example, have excited much interest over the last few decades owing to their importance in biology and ecology [1, 2] and to their potential uses in technological applications [3–5]. Such 'active' suspensions differ from their passive counterparts in that self-propelled particles inject energy into the suspending fluid as they move, resulting in unusual and complex dynamics even in the absence of any external forcing. Experiments have demonstrated that this fundamental difference can result in concentration patterns and complex fluid motions akin to high-Reynolds-number turbulence [6–8], which in turn are responsible for enhanced particle diffusion and fluid mixing [4, 9]. These dynamics have also been observed in simulations [10–16], and have been explained as the nonlinear consequence of flow instabilities driven by the particles [12, 13].

In addition to the dynamics that these suspensions exhibit, their rheology is also of interest. As it propels itself, a swimming particle is known to exert a net force dipole on the surrounding fluid [10, 13] as a result of the balance between the propulsive force exerted by the particle and the viscous drag on its body. This force dipole, of magnitude σ_0, can be of either sign depending on the mechanism for swimming: a *pusher* particle, which propels itself by exerting a force near its tail, will result in $\sigma_0 < 0$, whereas a *puller* particle, which swims using its head, will result in $\sigma_0 > 0$. In both cases, the dipole induces a disturbance flow around the particle, which results in hydrodynamic interactions and is responsible for the dynamics described above.

In addition, we also expect it to modify the effective rheology of the suspension.

This observation was previously made by Hatwalne et al. [17], who generalized kinetic equations for liquid crystals to model the rheology of active suspensions. Their linear viscoelastic theory predicted a decrease in the effective viscosity in the case of pushers (and an increase for pullers). More recently, Ishikawa and Pedley [18] performed Stokesian dynamics simulations of suspensions of spherical 'squirmers', that swim as a result of a prescribed slip velocity on their surface. In the dilute limit, they found no change in effective viscosity due to swimming (for non-bottom heavy particles), a consequence of the spherical shape they assumed, which results in an isotropic orientation distribution. Using analytical calculations, Haines et al. [19] indeed showed that if the orientation distribution is assumed to be anisotropic, swimming does result in a change in viscosity: using an *ad hoc* orientation distribution, they also observed a decrease in viscosity in suspensions of pushers.

In this work, we present a simple kinetic model for the shear rheology of a dilute suspension of self-propelled particles. Neglecting particle-particle hydrodynamic interactions, we extend previous work on passive particle suspensions [20–26] to the case of active suspensions. Numerical solutions for the orientation distribution of a single rod in simple shear flow are obtained from first principles by solving a Fokker-Planck equation, and are used to calculate the particle extra stress as an average over orientations of the force dipoles on the particles, which include contributions from the external flow, Brownian rotations, and the permanent dipole arising from swimming. The effects of flow strength, rotary diffusion and particle tumbling, all of which affect the orientation distribution of the particles, are analyzed in detail.

Kinetic Model

We consider the dynamics of a single swimming particle placed in a simple shear flow with velocity field $\mathbf{u}(\mathbf{x}) = \dot{\gamma}\, y\, \hat{\mathbf{x}}$, as depicted in Fig. 1. We denote by $\mathbf{p}$ the particle director, which is a unit vector defining the particle orientation and swimming direction relative to the external flow. The configuration of the particle may be represented by a distribution function $\Psi(\mathbf{p})$, which satisfies the Fokker-Planck equation [27]

$$\frac{\partial \Psi}{\partial t} + \nabla_{\mathbf{p}} \cdot (\dot{\mathbf{p}}\Psi) - d_r \nabla_{\mathbf{p}}^2 \Psi + \frac{1}{\tau}\left(\Psi - \frac{1}{4\pi}\right) = 0, \qquad (1)$$

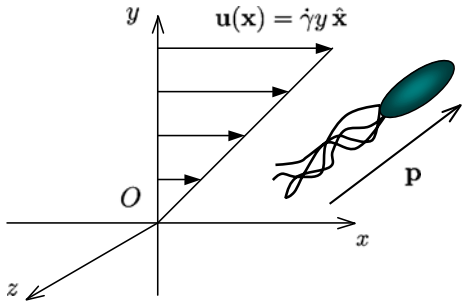

Fig. 1 Shear flow of an active suspension. The particle director $\mathbf{p}$ indicates the orientation of the particles and direction of swimming relative to the external flow

where $\nabla_{\mathbf{p}}$ is the gradient operator on the surface of the unit sphere S. The distribution function is normalized by

$$\int_S \Psi(\mathbf{p})\, d\mathbf{p} = 1, \qquad (2)$$

which confers to $\Psi(\mathbf{p})$ a mean value of $1/4\pi$. In equation (1), $\dot{\mathbf{p}}$ denotes the rotational velocity of the particle resulting from the local shear flow, and may be modeled using Jeffery's equation [28, 29] as

$$\dot{\mathbf{p}} = (\mathbf{I} - \mathbf{pp}) \cdot (\beta \mathbf{E} + \mathbf{W}) \cdot \mathbf{p}, \qquad (3)$$

where $\mathbf{E} = (\nabla\mathbf{u} + \nabla\mathbf{u}^T)/2$ and $\mathbf{W} = (\nabla\mathbf{u} - \nabla\mathbf{u}^T)/2$ are the constant rate-of-strain and rate-of-vorticity tensors of the imposed flow, respectively, and β is a constant parameter between -1 and 1 characterizing the particle shape ($\beta \approx 1$ for a slender particle).

In equation (1), the third term on the left-hand side models rotary diffusion (with constant diffusivity d_r), which may arise as a result of Brownian fluctuations or may also model hydrodynamic rotary diffusion resulting from hydrodynamic interactions [10, 11]. Finally, the last term in equation (1), first proposed by Subramanian and Koch [30], is used to model particle tumbling as a Poisson process, with characteristic correlation time τ.

A few comments on the validity of the Fokker-Planck equation (1) are in order. The description of the configuration of the suspension in terms of an orientation distribution $\Psi(\mathbf{p})$ implicitly assumes that the suspension is homogeneous in space, which is a valid approximation in the limit of infinite diluteness. Indeed, particle simulations [10, 11, 15] have shown that at low volume fractions swimming particles undergo ballistic motions for most of the time, except for rare particle-particle encounters during which their orientations change, resulting in an effective rotary diffusion over long times. In this regime, the spatial distribution of the particles may be considered homogeneous, and

the configuration of the suspension is therefore well captured by a Fokker-Planck equation for the orientation distribution with an effective rotary diffusivity, as in equation (1). While in a real system this diffusivity will be a function of concentration [10, 11], we here assume for simplicity that it is a constant; including the dependence on concentration would be straightforward and would not modify the formalism described here. If the concentration was to be increased beyond the dilute limit, complex spatial distributions may also arise as a result of hydrodynamic interactions [11–14] and could only be accounted for through a more sophisticated model, e.g. [13].

Once the orientation distribution $\Psi(\mathbf{p})$ is known by solution of equation (1), it can be used to evaluate the stress tensor in the suspension. The total stress $\boldsymbol{\Sigma}$ is expressed as the sum of the Newtonian stress and of a particle extra stress:

$$\boldsymbol{\Sigma} = -q\mathbf{I} + 2\mu\mathbf{E} + \boldsymbol{\Sigma}^p, \tag{4}$$

where q denotes the fluid pressure and μ is the dynamic viscosity of the suspending fluid. Following the classical theories of Batchelor [20] and Hinch and Leal [23], we define the extra stress $\boldsymbol{\Sigma}^p$ as the configuration average of the force dipoles $\mathbf{S}(\mathbf{p})$ exerted by the particles on the fluid, which in the dilute limit is given by:

$$\boldsymbol{\Sigma}^p = n\langle \mathbf{S}(\mathbf{p})\rangle = n\int_S \mathbf{S}(\mathbf{p})\Psi(\mathbf{p})\,d\mathbf{p}, \tag{5}$$

where n is the number density of the suspension. It can further be decomposed as the sum of three contributions, arising from the external flow, Brownian rotations, and the permanent dipole due to swimming:

$$\boldsymbol{\Sigma}^p = \boldsymbol{\Sigma}^f + \boldsymbol{\Sigma}^b + \boldsymbol{\Sigma}^s. \tag{6}$$

The first two contributions also arise with passive particles and were obtained previously as [24]

$$\boldsymbol{\Sigma}^f = nA\left[\langle \mathbf{pppp}\rangle - \frac{\mathbf{I}}{3}\langle \mathbf{pp}\rangle\right] : \mathbf{E}, \tag{7}$$

$$\boldsymbol{\Sigma}^b = 3nkT\left[\langle \mathbf{pp}\rangle - \frac{\mathbf{I}}{3}\right], \tag{8}$$

where $\langle \mathbf{pp}\rangle$ and $\langle \mathbf{pppp}\rangle$ denote the second and fourth moments of $\Psi(\mathbf{p})$ with respect to $\mathbf{p}$. In equation (7), A is a constant that depends on the particle shape. In this work, we consider the case of a slender rod of length L and inverse aspect ratio ϵ, for which it can be evaluated using slender-body theory as $A = \pi\mu L^3/6\log(2/\epsilon)$ [24]. In equation (8), kT denotes the thermal energy of the fluid (or effective thermal energy if rotary diffusion is used to model hydrodynamic diffusion). Finally, the component of the stress resulting from the permanent dipole due to swimming can be expressed as [12, 13]

$$\boldsymbol{\Sigma}^s = n\sigma_0\left[\langle \mathbf{pp}\rangle - \frac{\mathbf{I}}{3}\right], \tag{9}$$

where the dipole magnitude σ_0 is a constant that depends on the precise mechanism for swimming and can be interpreted as a measure of activity. For tail-actuated swimmers or *pushers*, $\sigma_0 < 0$, whereas for head-actuated swimmers or *pullers*, $\sigma_0 > 0$. It can be shown from micromechanical models for single swimmers that σ_0 is related to the swimming speed U_0 by a relation of the type $\sigma_0/\mu U_0 L^2 = \alpha$, where α is a dimensionless constant of same sign as σ_0. Note that the level of approximation of equations (7)–(9) is consistent with the neglect of hydrodynamic interactions in the Fokker-Planck equation (1), as it can be shown that such interactions would result in $O(n^2)$ corrections to the stress tensor (equation (5)).

We non-dimensionalize the equations using the following characteristic scales for stresses and times:

$$\Sigma_c = n|\sigma_0|, \quad \text{and} \quad t_c = \frac{\pi\mu L^3}{6|\sigma_0|\log(2/\epsilon)}. \tag{10}$$

The time scale t_c can be interpreted as the characteristic time for a particle to drag fluid along its length under the effect of its permanent force dipole, or equivalently as a characteristic time scale for swimming (owing to the relationship between σ_0 and U_0). We also define the dimensionless rate of strain, rotary diffusivity and correlation time as:

$$\tilde{\dot\gamma} = \dot\gamma t_c, \quad \tilde{d}_r = d_r t_c, \quad \tilde\tau = \tau/t_c. \tag{11}$$

With these notations, the steady-state Fokker-Planck equation (1) becomes

$$\tilde{\dot\gamma}\nabla_{\mathbf{p}}\cdot(\dot{\mathbf{p}}\Psi) - \tilde{d}_r\nabla^2_{\mathbf{p}}\Psi + \frac{1}{\tilde\tau}\left(\Psi - \frac{1}{4\pi}\right) = 0, \tag{12}$$

where $\dot{\mathbf{p}}$ has been scaled by $\dot\gamma$. Note that the steady-state orientation distribution really only depends on two dimensionless groups, namely $\tilde{\dot\gamma}/\tilde{d}_r$ (which can be interpreted as a rotary Péclet number) and $\tilde{\dot\gamma}\tilde\tau$. Equation (12) was solved numerically using a spectral expansion of the distribution $\Psi(\mathbf{p})$ on the basis of spherical harmonics, in a similar way as in the work of Chen and Koch [25]. Harmonics of degree up to 40 were included, corresponding to a total of 861 modes and ensuring an excellent accuracy over the range of parameters

considered here. Typical orientation distributions for a few values of $\tilde{\dot{\gamma}}/\tilde{d}_r$ and $\tilde{\dot{\gamma}}\tilde{\tau}$ are shown in Fig. 2, where we find as expected that an increase in flow strength causes the particles to align in the flow direction, whereas both rotary diffusion and tumbling tend to randomize the distributions.

Once the distributions are known, they can be used to evaluate the particle extra stress using equations (6)–(9). In dimensionless form,

$$\tilde{\boldsymbol{\Sigma}}^p = \tilde{\dot{\gamma}}\left[\langle \mathbf{pppp}\rangle - \frac{\mathbf{I}}{3}\langle \mathbf{pp}\rangle\right] : \mathbf{E} + (6\tilde{d}_r \pm 1)\left[\langle \mathbf{pp}\rangle - \frac{\mathbf{I}}{3}\right], \tag{13}$$

where the plus sign corresponds to the case of pullers ($\sigma_0 > 0$), whereas the minus sign corresponds to pushers ($\sigma_0 < 0$). Next, we present results for the dimensionless particle viscosity η_p, first normal stress difference coefficient ν_p, and second normal stress difference coefficient κ_p, defined by

$$\eta_p = \frac{\tilde{\Sigma}^p_{xy}}{\tilde{\dot{\gamma}}}, \quad \nu_p = \frac{\tilde{\Sigma}^p_{xx} - \tilde{\Sigma}^p_{yy}}{\tilde{\dot{\gamma}}^2}, \quad \kappa_p = \frac{\tilde{\Sigma}^p_{yy} - \tilde{\Sigma}^p_{zz}}{\tilde{\dot{\gamma}}^2}. \tag{14}$$

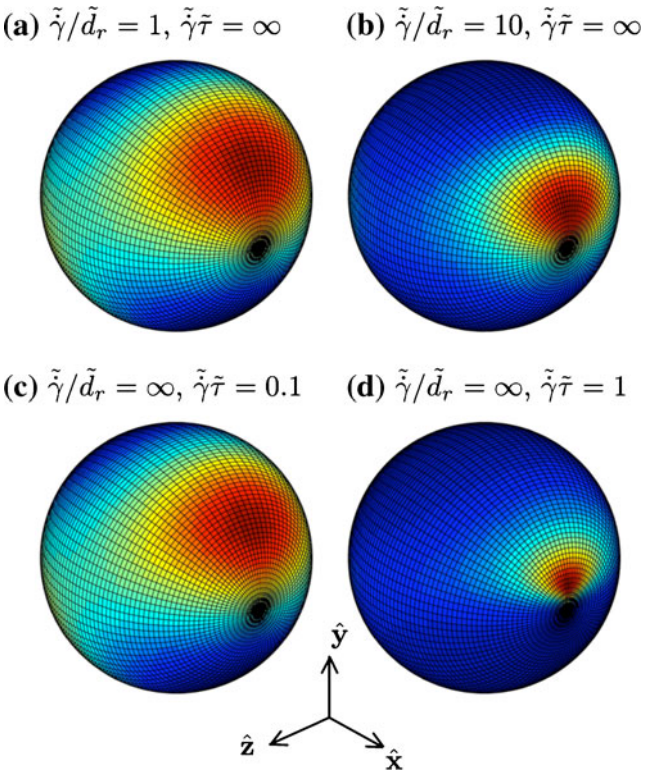

Fig. 2 Steady-state orientation distributions $\Psi(\mathbf{p})$ for the simple shear flow of a slender particle ($\beta = 1$) for various values of the two dimensionless groups $\tilde{\dot{\gamma}}/\tilde{d}_r$ and $\tilde{\dot{\gamma}}\tilde{\tau}$

Using equation (13), we find:

$$\eta_p = \langle p_x^2 p_y^2\rangle + \frac{(6\tilde{d}_r \pm 1)}{\tilde{\dot{\gamma}}}\langle p_x p_y\rangle, \tag{15}$$

$$\nu_p = \frac{\langle p_x^3 p_y\rangle - \langle p_x p_y^3\rangle}{\tilde{\dot{\gamma}}} + \frac{(6\tilde{d}_r \pm 1)}{\tilde{\dot{\gamma}}^2}\left(\langle p_x^2\rangle - \langle p_y^2\rangle\right), \tag{16}$$

$$\kappa_p = \frac{\langle p_x p_y^3\rangle - \langle p_x p_y p_z^2\rangle}{\tilde{\dot{\gamma}}} + \frac{(6\tilde{d}_r \pm 1)}{\tilde{\dot{\gamma}}^2}\left(\langle p_y^2\rangle - \langle p_z^2\rangle\right). \tag{17}$$

Results and Discussion

We first consider the case of smooth swimmers for which tumbling is negligible ($\tilde{\tau} = \infty$) in Fig. 3. Figure 3(a) shows the effective particle viscosity η_p versus dimensionless shear rate $\tilde{\dot{\gamma}}$ for both pushers and pullers and for various values of the rotary diffusivity $\tilde{d}_r$. In the case of *puller* particles (full symbols), we find that the viscosity is qualitatively similar to that of a suspension of passive Brownian rods [22, 24, 25], and in particular exhibits shear thinning. The effect of the rotary diffusivity is the clearest in weak flows, where an increase in $\tilde{d}_r$ is found to result in a decrease in the zero-shear-rate viscosity as a consequence of the randomization of the orientations, which reduces the contribution of the Brownian and permanent dipoles to the viscosity. In all cases, however, activity increases the viscosity of the suspension in the case of pullers: this effect could easily have been anticipated from equation (15), where we see that the permanent dipole due to swimming results in an effective enhancement of the Brownian contribution to the viscosity. The case of *pushers* (open symbols) is more interesting, as Fig. 3(a) shows that activity causes a significant decrease in the effective particle viscosity η_p, a result that once again could have been anticipated from equation (15). The effect is strongest in weak flows and even results in negative values of η_p for low values of the rotary diffusivity $\tilde{d}_r$ and low values of the shear rate $\tilde{\dot{\gamma}}$ (note that negative values of η_p are not unphysical, since η_p only represents the first correction to the Newtonian viscosity μ due to swimming). Both observations (increase in η_p for pullers and decrease for pushers) are also consistent with the previous predictions of Hatwalne et al. [17] and of Haines et al. [19].

These trends can be explained more precisely using an analytical expression for the zero-shear-rate viscosity η_p^0, which can be obtained from an asymptotic

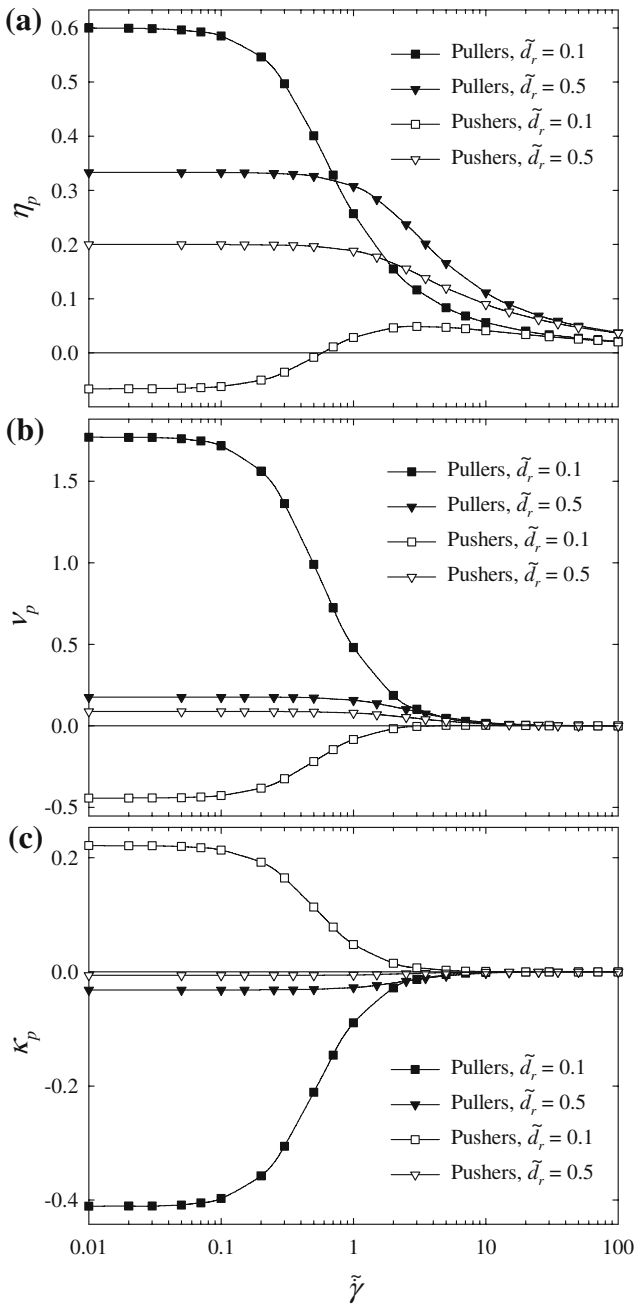

Fig. 3 Rheology of a suspension of smooth slender swimmers ($\beta = 1$, $\tilde{\tau} = \infty$): (**a**) effective viscosity η_p, (**b**) first normal stress difference coefficient ν_p, and (**c**) second normal stress difference coefficient κ_p versus dimensionless rate of strain $\tilde{\dot{\gamma}}$ for suspensions of pushers and pullers

solution of the Fokker-Planck equation (12) in the limit of $\tilde{\dot{\gamma}} \to 0$, and is given by

$$\eta_p^0 = \frac{1}{15}(1 + 3\beta) \pm \frac{\beta}{30\tilde{d}_r}, \tag{18}$$

in excellent quantitative agreement with the data of Fig. 3. The last term in equation (18) corresponds to the contribution from swimming. In particular, we find that activity always causes an increase in η_p^0 for pullers but a decrease for pushers, and that this effect is stronger for small values of $\tilde{d}_r$. Equation (18) also shows that for pushers, a negative particle viscosity will occur when $\tilde{d}_r < \beta/(2 + 6\beta)$, or $\tilde{d}_r < 1/8$ in the case of slender particles ($\beta = 1$). As seen in Fig. 3(a), this effective viscosity is only negative up to a certain critical flow strength $\tilde{\dot{\gamma}}_c$, beyond which it becomes positive again. This is illustrated more clearly in Fig. 4, showing the critical flow strength as a function of the rotary diffusivity: in particular, the range of flow strengths over which negative viscosities occur decreases with $\tilde{d}_r$, and altogether disappears when $\tilde{d}_r > 1/8$ in agreement with the analytical prediction.

Results for the first and second normal stress difference coefficients are also shown in Fig. 3(b) and (c). In the case of pushers, $\nu_p > 0$ and $\kappa_p < 0$ as in the case of passive rod suspensions, with extrema occurring at zero shear rate. We find however that swimming results in a strong increase in the magnitude of these coefficients with respect to the passive case. The case of pushers, once again, is more atypical, as it is found that the first normal stress difference coefficient ν_p is decreased and can even become negative at low values of $\tilde{d}_r$, whereas the second normal stress difference coefficient κ_p is increased and can become positive. For both types of suspensions, we find that the magnitude of both coefficients increases with decreasing diffusivity $\tilde{d}_r$ (or equivalently with increasing activity), a trend easily anticipated from equations (16) and (17).

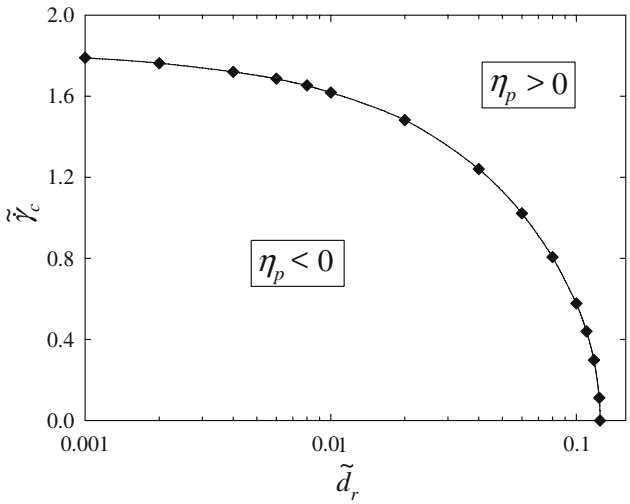

Fig. 4 Critical flow strength $\tilde{\dot{\gamma}}_c$ below which a suspension of smooth slender pushers ($\beta = 1$, $\tilde{\tau} = \infty$) exhibits a negative effective particle viscosity η_p, as a function of dimensionless diffusivity $\tilde{d}_r$. Negative viscosities only occur for $\tilde{d}_r < 1/8$, in agreement with the theoretical prediction of equation (18)

The effects of particle tumbling are shown in Fig. 5, where η_p, ν_p and κ_p are plotted versus flow strength for various values of the tumbling correlation time $\tilde{\tau}$ at a fixed value of the rotary diffusivity ($\tilde{d}_r = 0.1$). The main consequence of particle tumbling is to reduce the effects of activity on the rheology. Specifically, the viscosity η_p is reduced in the case of pullers and enhanced in the case of pushers, for which it even becomes positive again at sufficiently low values of $\tilde{\tau}$. Similarly, the magnitude of all the normal stress difference coefficients is reduced in the case of strong tumbling (or low values of $\tilde{\tau}$). These trends were to be expected, as tumbling results in a randomization of the orientations, and therefore in a reduction of the swimming stress $\mathbf{\Sigma}^s$, which is proportional to the nematic order parameter as seen in equation (9).

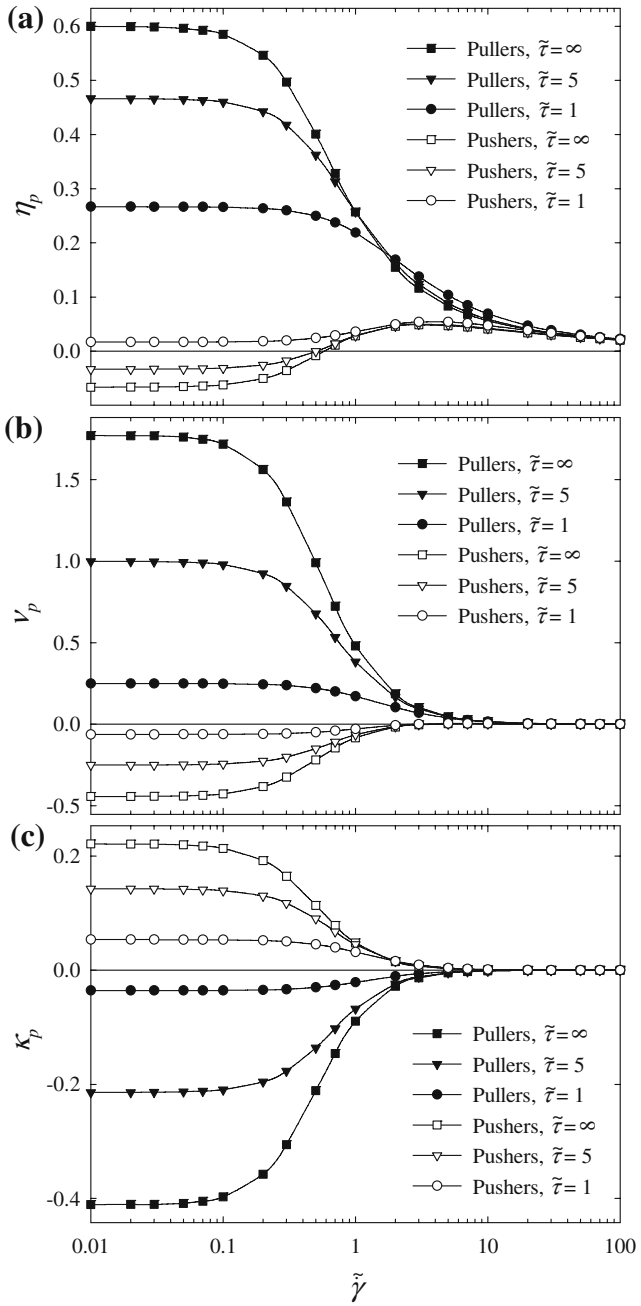

Fig. 5 Effect of tumbling on the rheology of a suspension of slender swimmers ($\beta = 1$): (**a**) effective viscosity η_p, (**b**) first normal stress difference coefficient ν_p, and (**c**) second normal stress difference coefficient κ_p versus dimensionless rate of strain $\tilde{\dot{\gamma}}$ for suspensions of pushers and pullers, for a rotary diffusivity of $\tilde{d}_r = 0.1$ and for various values of the tumbling correlation time $\tilde{\tau}$

In summary, the dilute kinetic theory presented here uncovered several interesting rheological properties of suspensions of swimming particles. In particular, we found that suspensions of pullers qualitatively behave like suspensions of passive particles, but with an increased effective viscosity and increased first and second normal stress differences. Suspensions of pushers are more atypical, and exhibit a strong decrease in viscosity due to activity, which can even result in a negative particle viscosity in weak flows. As discussed above, pushers can also exhibit a negative first normal stress difference coefficient and a positive second normal stress difference coefficient, in contrast with passive suspensions. These unusual results are quite interesting and make active suspensions of biological or artificial microswimmers prime candidates for use in applications requiring smart materials or fluids with tailored rheological properties.

The decreased particle viscosity in suspensions of pushers also bears implications for the dynamics of these suspensions, as it may result in flow destabilization in some applications. In particular, it has been conjectured [30, 31] that this decrease in viscosity is responsible for the flow instabilities and chaotic dynamics that have been observed in both experimental [7] and computational [11–13] studies of these systems.

An important assumption of the present theory is the diluteness of the suspension, which allowed us to neglect the spatial dependence of the distribution function Ψ and to assume that the orientation distribution is entirely determined by the external flow field. When hydrodynamic interactions are taken into account, active suspensions in the absence of external forcing are known to exhibit complex flows and coherent structures [13]: it is unclear how these structures would evolve in an external flow, nor how they would influence the effective rheology of the suspensions. Answering these important open questions will require improvements upon the present theory to include these effects, for instance by adapting the more general kinetic model proposed by Saintillan and Shelley [12, 13] to the case of flowing suspensions: this will be the subject of future work.

Acknowledgement The author would like to thank Michael Shelley for useful conversations on this work.

References

1. Hill NA, Pedley TJ (2005) Bioconvection. Fluid Dyn Res 37:1–20
2. Kils U (1993) Formation of micropatches by zooplankton-driven microturbulences. Bull Mar Sci 53:160–169
3. Paxton WF, Kistler KC, Olmeda CC, Sen A, St Angelo SK, Cao Y, Mallouk TE, Lammert PE, Crespi VH (2004) Catalytic nanomotors: autonomous movement of striped nanorods. J Am Chem Soc 126:13424
4. Kim MJ, Breuer KS (2004) Enhanced diffusion due to motile bacteria. Phys Fluids 16:L78
5. Darnton N, Turner L, Breuer K, Berg HC (2004) Moving fluid with bacterial carpets. Biophys J 86:1863–1870
6. Mendelson NH, Bourque A, Wilkening K, Anderson KR, Watkins JC (1999) Organized cell swimming motions in *Bacillus subtilis* colonies: patterns of short-lived whirls and jets. J Bacteriol 181:600
7. Dombrowski C, Cisneros L, Chatkaew S, Goldstein RE, Kessler JO (2004) Self-concentration and large-scale coherence in bacterial dynamics. Phys Rev Lett 93:098103
8. Cisneros LH, Cortez R, Dombrowski C, Wolgemuth CW, Kessler JO, Golstein RE (2007) Fluid dynamics of self-propelled microorganisms, from individuals to concentrated populations. Exp Fluids 43:737–753
9. Wu XL, Libchaber A (2000) Particle diffusion in a quasi-two-dimensional bacterial bath. Phys Rev Lett 84:3017
10. Hernández-Ortiz JP, Stoltz CG, Graham MD (2005) Transport and collective dynamics in suspensions of confined self-propelled particles. Phys Rev Lett 95:203501
11. Saintillan D, Shelley MJ (2007) Orientational order and instabilities in suspensions of self-locomoting rods. Phys Rev Lett 99:058102
12. Saintillan D, Shelley MJ (2008) Instabilities and pattern formation in active particle suspensions: kinetic theory and continuum simulations. Phys Rev Lett 100:178103
13. Saintillan D, Shelley MJ (2008) Instabilities, pattern formation and mixing in active suspensions. Phys Fluids 20:123304
14. Ishikawa T, Locsei JT, Pedley TJ (2008) Development of coherent structures in concentrated suspensions of swimming model micro-organisms. J Fluid Mech 615:401–431
15. Mehandia V, Nott PR (2008) The collective dynamics of self-propelled particles. J Fluid Mech 595:239–264
16. Wolgemuth CW (2008) Collective swimming and the dynamics of bacterial turbulence. Biophys J 95:1564–1574
17. Hatwalne Y, Ramaswamy S, Rao M, Aditi Simha R (2004) Rheology of active-particle suspensions. Phys Rev Lett 92:118101
18. Ishikawa T, Pedley TJ (2007) The rheology of a semi-dilute suspension of swimming model micro-organisms. J Fluid Mech 588:399–435
19. Haines BM, Aranson IS, Berlyland L, Karpeev DA (2008) Effective viscosity of dilute bacterial suspensions: a two-dimensional model. Phys Biol 5:1–9
20. Batchelor GK (1974) Transport properties of two-phase materials with random structure. Annu Rev Fluid Mech 6:227–255
21. Hinch EJ, Leal LG (1972) The effect of Brownian motion on the rheological properties of a suspension of non-spherical particles. J Fluid Mech 52(4):683–712
22. Brenner H (1974) Rheology of a dilute suspension of axisymmetric Brownian particles. Int J Multiph Flow 1:195–341
23. Hinch EJ, Leal LG (1975) Constitutive equations in suspension mechanics. Part 1. General formulation. J Fluid Mech 71(3):481–495
24. Hinch EJ, Leal LG (1976) Constitutive equations in suspension mechanics. Part 2. Approximate forms for a suspension of rigid particles affected by Brownian rotations. J Fluid Mech 76(1):187–208
25. Chen SB, Koch DL (1996) Rheology of dilute suspensions of charged fibers. Phys Fluids 8(11):2792–2807
26. Chen SB, Jiang L (1999) Orientation distribution in a dilute suspension of fibers subject to simple shear flow. Phys Fluids 11(10):2878–2890
27. Doi M, Edwards SF (1986) The theory of polymer dynamics. Oxford University Press, Oxford
28. Jeffery GB (1922) The motion of ellipsoidal particles immersed in a viscous fluid. Proc R Soc Lond Ser A 102:161
29. Bretherton FP (1962) The motion of rigid particles in a shear flow at low Reynolds number. J Fluid Mech 14:284
30. Subramanian G, Koch DL (2009) Critical bacterial concentration for the onset of collective swimming. J Fluid Mech (in press)
31. Underhill PT, Hernandez-Ortiz JP, Graham MD (2008) Diffusion and spatial correlations in suspensions of swimming particles. Phys Rev Lett 100:248101